Proc. AIAA Atmospheric Flight Mechanics Conference
AIAA-2011-6459, 20 pages, Portland, OR, USA (2011)

Suppression of the Aeroelastic/Aeroservoelastic Interaction Using Adaptive Feedback Control Instead of Notching Filters

Jie Zeng*
and Jiang Wang†
ZONA Technology Inc, Scottsdale, Arizona, 85258, U.S.A

Raymond de Callafon‡
University of California, San Diego, La Jolla, California, 92093, U.S.A

Martin Brenner§
NASA Dryden Flight Research Center, Edwards, California, 93523, U.S.A

This paper investigates the possibility that an adaptive feedback controller can be designed and implemented for the suppression of aircraft's structural vibration in the presence of any aeroelastic/aeroservoelastic interaction, instead of using the non-adaptive notching filters. Currently aircraft with non-adaptive control laws usually include roll-off or notch filters to avoid AE/ASE interactions. However, if changes in the aircraft configuration are significant, the frequencies of the flexible modes of the aircraft may be shifted and the notch filters could become totally ineffective. With the proposed adaptive feedback control technology, the flexible dynamics can be consistently estimated via system identification algorithms and its undesirable effects are suppressed through a robust feedback control law, while the whole systems stability is being maintained. The proposed feedback control technique is demonstrated with a 6-DOF nonlinear F/A-18 AAW model for the suppression of the aeroelastic/aeroservoelastic interaction.

I. Introduction

To date, because of the slender, more flexible, and/or sizable design of the next generation aircraft such as Morphing UAVs, HALEs, Oblique Flying Wings, sensorcrafts, etc., where there is insufficient frequency separation between the rigid body dynamics and relatively low frequency aeroelastic/aeroservoelastic modes, flight control laws based on the 6 d.o.f. rigid body model may result in unacceptable stability margins or undesirable response characteristics due to control input or turbulence. Therefore, to maintain good flying qualities of an aircraft, the aeroelastic/aeroservoelastic modes interaction to the rigid body dynamics has to be minimized using appropriate methods.

The usual way to suppress the effects of the low frequency aeroelastic/aeroservoelastic modes on the rigid body dynamics was performed through the notch filter design technique. However, if changes in the aircraft configuration are significant, the frequencies of the flexible modes of the aircraft may be shifted and the notch filters could become totally ineffective.

In this paper an indirect adaptive control algorithm is introduced to suppress the aeroelastic/aeroservoelastic modes interaction. With this algorithm, poorly damped structural resonance modes induced by aero(servo)elastic interaction can be monitored and modelled via system identification techniques. Such estimation techniques can use time-domain measurements of input/output behavior to formulate a dynamical model suitable for control system design for vibration suppression. With the availability of a model, a model-based feedback control design methodology can be used to dampen the resonance modes, and therefore reduce the the effects of the aeroelastic/aeroservoelastic modes on rigid

*R & D Control System Engineer, Member AIAA. jzeng@zonatech.com
†Member AIAA. jwang@zonatech.com
‡Associate Professor. calafon@ucsd.edu
§Aerospace Engineer, Member AIAA. Martin.J.Brenner@nasa.gov

body dynamics. The performance of the notch filters and the proposed adaptive control algorithm are compared and validated with the use of the nonlinear F/A-18 AAW model integrated with the NASA AAW flight research controller.

II. Adaptive Control Algorithm

The adaptive control algorithm implemented in this paper includes two part: aeroelastic/aeroservoelastic model approximation using system identification techniques and robust controller design based on the estimated aeroelastic/aeroservoelastic model for the suppression of the aeroelastic/aeroservoelastic interaction.

Aeroelastic/Aeroservoelastic Model Approximation

Consider a linear, time-invariant, discrete-time system

$$y(t) = \sum_{k=0}^{\infty} G(k)u(t-k) + v(t). \tag{1}$$

The system Markov parameters, $G(k) \in \mathbb{R}^{n_y \times n_u}$ define the relationship between the input signal, $u(t) \in \mathbb{R}^{n_u}$, and the output signal, $y(t) \in \mathbb{R}^{n_y}$, which contains an additive noise signal, $v(t) \in \mathbb{R}^{n_y}$. We assume that the input and output signals are quasi-stationary and that the noise, $v(t)$, is stationary.

Such a system has an infinite number of state-space representations of the form

$$\begin{aligned} x(t+1) &= Ax(t) + Bu(t) \\ y(t) &= Cx(t) + Du(t) + v(t) \end{aligned} \tag{2}$$

given in terms of constant matrices $A \in \mathbb{R}^{n \times n}$, $B \in \mathbb{R}^{n \times n_u}$, $C \in \mathbb{R}^{n_y \times n}$, and $D \in \mathbb{R}^{n_y \times n_u}$. The state-space matrices are related to the system Markov parameters by $G(k) = CA^{k-1}B$ for $k > 0$ and $G(0) = D$. We assume that all state-space representations are controllable and observable, and that they are minimal, that is the dimension of the state equal to the system order n. The identification problem considered is to estimate (i) the system order n and (ii) state-space matrices A, B, C, and D from measured data generated by the above system. The problem of estimating a realization of the process that generates $v(t)$ is not addressed. With the input signal $u(t)$ and output signal $y(t)$ available, a time domain Subspace identification method[1] or step based system identification method[2] can be directly applied for the estimation of the system matrices A, B, C, and D.

H_∞ Loop Shaping Controller Design Method

The H_∞ loop shaping controller design method was developed by Glover and McFarlane.[3] This method is favorable as it formulates the control design problem as a standard 4-block problem for which an explicit solution exists based on a Nehari-extension. The computation of the controller does not require an iteration and solutions are formulated in the form of a Hankel-norm based model reduction for which standard Algebraic Ricatti equations need to be solved. The H_∞ loop shaping control design formulation is illustrated in Figure 1.

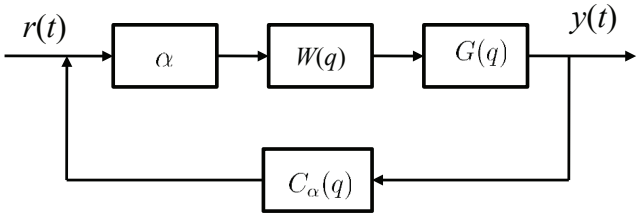

Figure 1. H_∞ Loop Shaping Control Design Formulation.

Essential to the automatic updating of the controller is the use of a loop shaping in the controller design methodology that allows the computation of controllers $C_{pert}(q)$ that are, by themselves, also stable. The loop shaping can be user specified or scaled by a scalar variable for automatic scaling selection to obtain a stable, stabilizing feedback controller. The scaling serves as an H_∞ loop shaping in the computation of the optimal controller as follows.

1. Define a weighted closed-loop model, $G_\alpha(q)$, given by

$$G_\alpha(q) = \alpha W(q) G(q)$$

where α is a variable gain and $W(q)$ is a fixed filter that can be used to specify high frequency roll-off or other desirable properties for the to-be computed controller $C_{pert}(q)$. $G(q)$ is the identified model which models the transient behavior of the resonance of the structure.

2. Solve the (weighted) 4-block H_∞ optimization problem

$$C_\alpha = \min_C \|T(G_\alpha, C)\|_\infty,\ T(G_\alpha, C) = \begin{bmatrix} G_\alpha \\ I \end{bmatrix} (I + CG_\alpha)^{-1} \begin{bmatrix} I & C \end{bmatrix}$$

The optimization is guaranteed to find a controller, C_α, that forms a stable feedback connection with G_α.

3. Check if the controller $C_\alpha(q)$ by itself is also stable. If not, reduce the value of α and go back to Item 1.

4. If the controller $C_\alpha(q)$ by itself is also stable, then compute C_{pert} via

$$C_{pert}(q) = \alpha W(q) C_\alpha(q)$$

The resulting controller $C_{pert}(q)$ will (internally) stabilize $G(q)$ and is by itself also stable. Stability of $C_{pert}(q)$ facilitates the on-line implementation of the controller as an additive perturbation to the original flight controller.

It should be noted that the H_∞ loop shaping controller design does not have the capability to explicitly deal with the structure vibrations due to the external unmeasurable perturbation such as gust perturbation.

III. Effects of the Notch Filters on the Reduction of the Aeroelastic/Aeroservoelastic Modes Interaction

In order to evaluate the effects of the notch filters on the suppression of the aeroelastic/aeroservoelastic modes interaction, and also investigate the feasibility of the H_∞ Controller replacing the noth filters for aeroelastic/aeroservoelastic vibration suppression, the NASA active aeroelastic wing (AAW) flight control system has been integrated into the current Nonlinear F/A-18 AAW simulink model. The integrated F/A-18 AAW model is illustrated in Figure 2. The NASA AAW flight control system in Figure 2 is marked by a red colored ellipse. One notch filter located at 9.55 Hz was added to the longitudinal control system, see Figure 3; and three additional notch filters located at 5 Hz, 7 Hz and 17 Hz were added to the lateral control system, see Figure 4. In the following sections, the integrated F/A-18 AAW closed loop linear model will be implemented to analyze the effects of the notch filters and H_∞ aeroelastic control on the aeroelastic/aeroservoelastic modes suppression.

The effects of the notch filters can be validated by turning on/off the notch filters in the longitudinal and lateral control system. In this study, only the longitudinal dynamics were focused on during the study of the aeroealstic/aeroservoelastic interaction. At flight condition M = 0.85, H = 15 Kft, injecting a doublet command to the longitudinal stick, by turning on/off the notch filters, the simulation results can be compared and further illustrated in Figures 5, 6, and 7. From the deflection of the control surfaces in Figure 7, normal acceleration responses at the C.G. position in Figure 6 (a) and (b), and pitch rate response in Figure 5(d), it is easily observed that with the use of the notch filter in the flight control system the aeroelastic/aeroservoelastic modes interaction can be successfully suppressed. However, from Figure 6 (a) and (b) it is clearly seen that the notch filters have no effects on the high frequency oscillation reduction of the normal acceleration response at left/right wing folder position, Nz_{km023L} and Nz_{km023R}. By further investigation it was found that the normal acceleration responses at the left/right wing folder position, Nz_{km023L} and Nz_{km023R}, were dominated by two elastic modes located at 6 Hz and 16.3 Hz, respectively. However, other high frequency responses such as Nz_{Plt} and Nz_{SNS} are dominated by an elastic mode around 9.5 Hz. That is the reason why with a notch filter at 9.55 Hz, the high frequency responses at the longitudinal direction can be successfully suppressed.

It is well known that using the notch filters in the control paths to suppress the presence of any undesired elastic modes is a standard automatic control practice in the aerospace industry. However, if changes in the aircraft configuration are significant, due to any abrupt operating conditions change, such as an unexpected massive store separation and/combat related structural damage, the frequencies of the flexible modes of the aircraft may be shifted and the notch filters could become totally ineffective. Under such circumstances, an adaptive control scheme through iteratively on-line estimating the aeroelastic/aeroservoelastic dynamics and design of the H_∞ aeroelastic controller for aeroelastic/aeroservoelastic modes interaction suppression will overcome the issues arising from the usage of the notch filters. In the following section, instead of using notch filters, a H_∞ aeroelastic controller is designed based on the model estimated using the system identification techniques, and its performance will be evaluated.

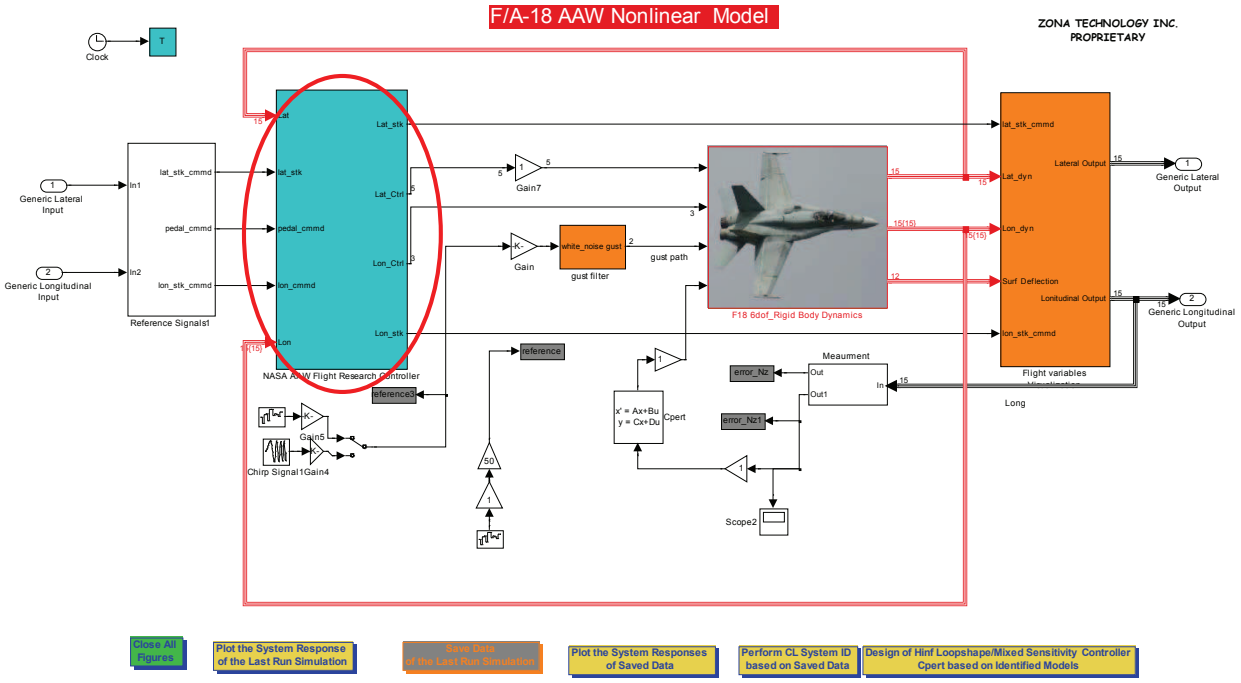

Figure 2. Integration of the NASA Flight Control System into F/A-18 AAW Nonlinear Model.

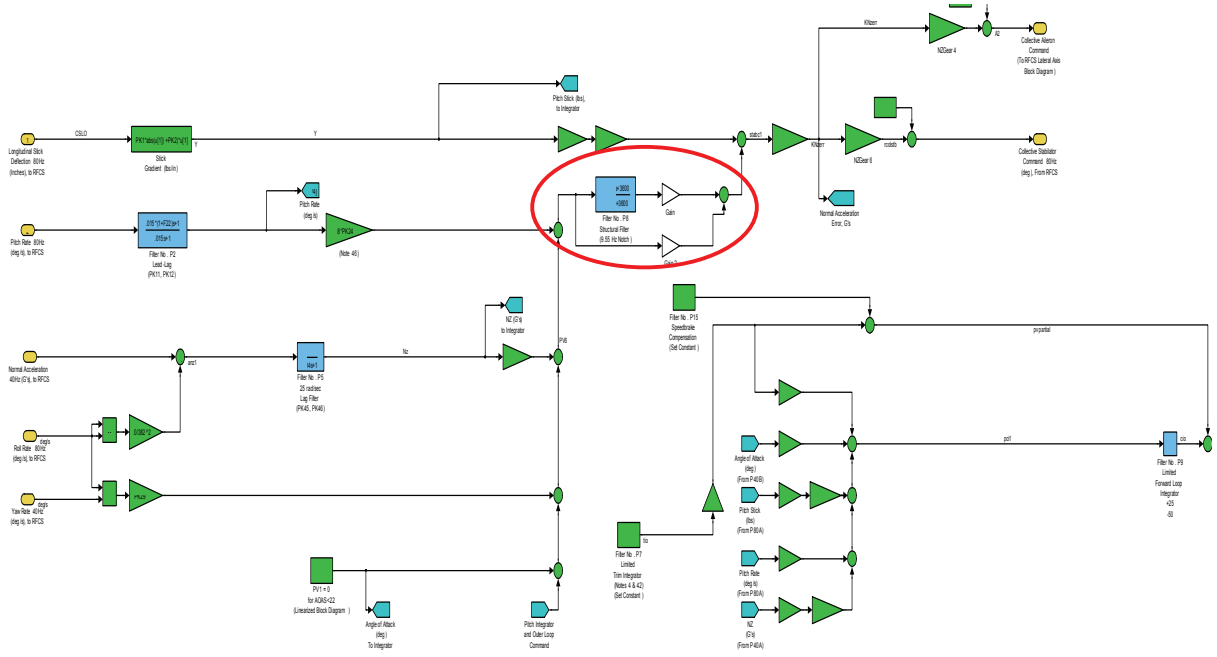

Figure 3. Longitudinal Flight Control System with Notch Filter at 9.55 Hz.

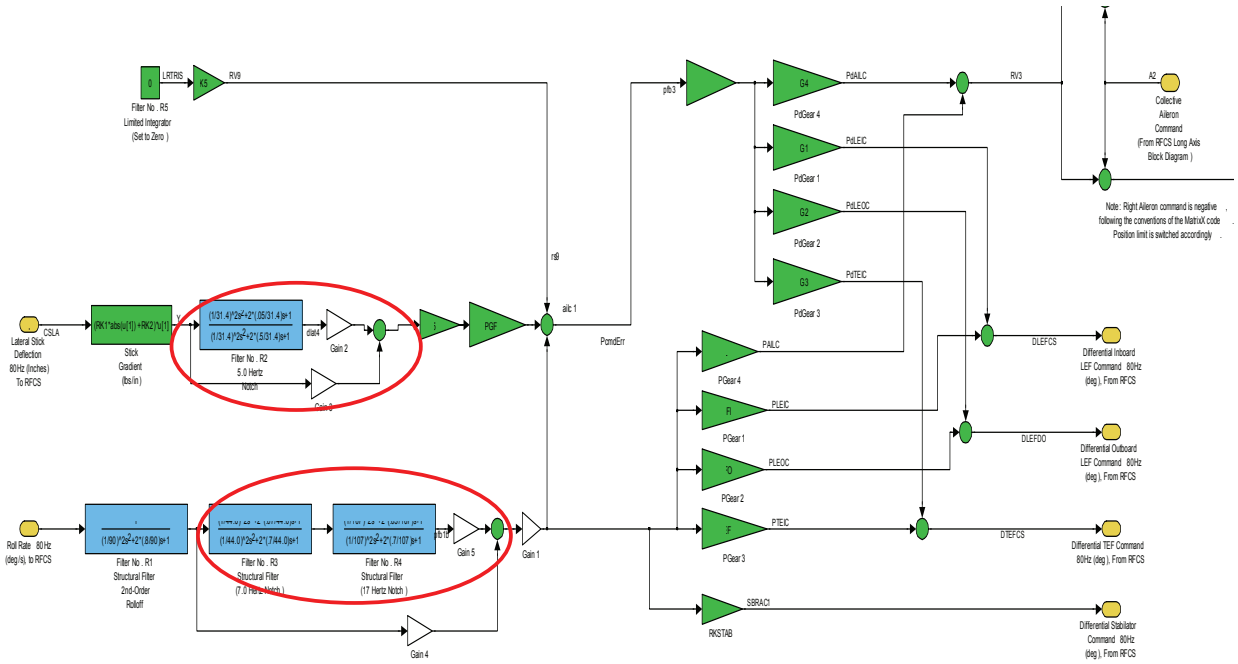

Figure 4. Longitudinal Flight Control System with Notch Filters at 5.0 Hz, 7.0 Hz and 9.55 Hz.

IV. H_∞ Control for Vibration Suppression without Notch Filter In the Loop

To investigate the possibility of using a feedback controller to replace the notch filter. Following steps are considered:

1. At the flight simulation condition M = 0.85, H = 15 Kft, injecting a step input to the collective trailing edge flapron, and collecting the acceleration response Nz_{SNS}, a low order aeroelastic model is estimated using the step based identification method.[2]

2. With the estimated low order aeroelastic model, a robust controller is then designed using H_∞ loopshaping control design method.

3. The performance of the designed controller is validated at three different flight simulation condition: M = 0.85, 0.9, and M= 0.95 (H = 15 Kft).

H_∞ Control Design at M = 0.85, H = 15 Kft

From the previous study we know that the notch filters have significant effects on the normal accelerations at the C.G. position. Therefore, for comparison purposes, during the aeroelastic/aeroservoelastic model estimation and H_∞ control design process, the normal acceleration response from the sensor location, Nz_{SNS}, is used for model estimation and feedback control design. Furthermore, the collective trailing edge flapron is used as the actuator to feedback the control signal. To eliminate the effects from the notch filters, all the notch filters will be turned off during the H_∞ control process.

By injecting a step input to the collective trailing edge flapron, and collecting the response Nz_{SNS} and input step signal, a 10th order aeroelastic/aeroservoelastic model is estimated. With the use of the estimated model, a H_∞ controller can be designed using the loop shaping H_∞ control design algorithms. To minimize the effects of the aeroelastic controller on the rigid body dynamics, a bandpass filter is implemented as the weighting function during the control process, using the control design framework shown in Figure 1. Figure 8 evaluates the aeroelastic modes suppression using the H_∞ controller on the estimated model. Figure 8(a) presents the designed bandpass filter W used for control design; Figure 8(b) shows the frequency domain plot of the resulting controller. It is seen from Figure 8 (c)

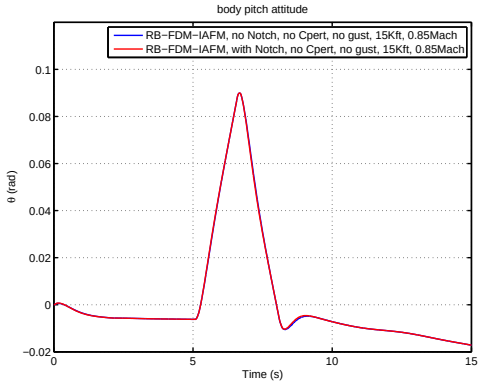

(a) Pitch Angle, $\theta(t)$.

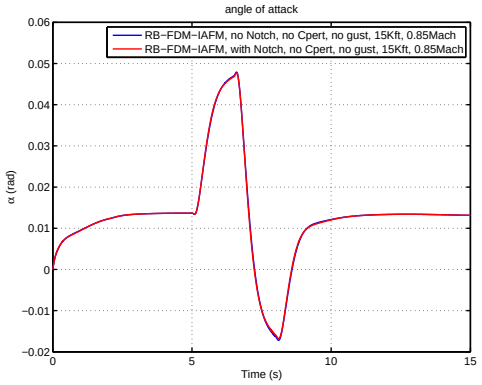

(b) Angle of Attach, $\alpha(t)$.

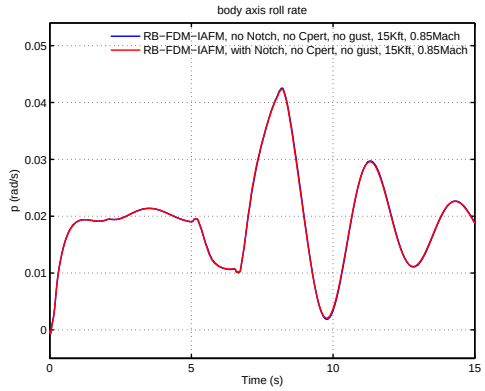

(c) Roll Rate, $p(t)$.

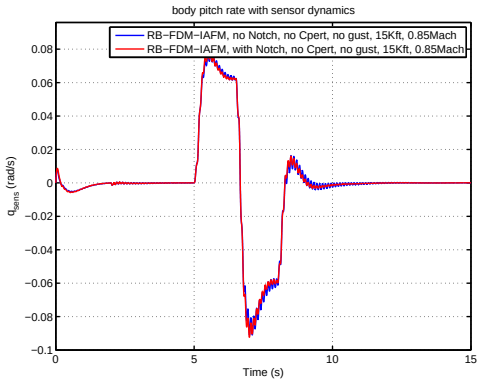

(d) Pitch Rate, $q(t)$.

Figure 5. Closed Loop Response of the Linear F/A-18 AAW Aeroelastic Model With/Without Notch Filters at M = 0.85, H = 15 Kft (Longitudinal Stick Command).

that the peak located at 9.5 Hz is successfully reduced. The time domain response in Figure 8 (d) further validates the effectiveness of the H_∞ controller.

Performance Validation of the H_∞ Controller at M = 0.85, H = 15 Kft

Implementing the designed H_∞ controller to the F/A-18 AAW nonlinear simulink model, the simulation results are plotted in Figures 9, 10, and 11. The simulation results without using the H_∞ controller are also plotted in the same figures for comparison. From these plots, it is clearly seen that:

- The vibration responses induced by the 9.5 Hz aeroelastic mode are successfully suppressed with the use of the H_∞ feedback controller.
- The H_∞ feedback controller has little influence on the rigid dynamics response.
- The H_∞ feedback controller cannot reduce the vibration response of the normal acceleration at wing folder position, Nz_{km023R} and Nz_{km023L}. To reduce the vibration responses of both Nz_{km023R} and Nz_{km023L}, an additional control activity should be considered.

Performance Validation of the H_∞ Controller at M = 0.90, H = 15 Kft

At flight simulation condition M = 0.90, H = 15 Kft, the simulation results with the feedback controller in the loop are plotted in Figures 12, 13, and 14. The simulation results obtained at M = 0.90, H = 15 Kft are similar as those at M = 0.85, H = 15 Kft. It is also observed that:

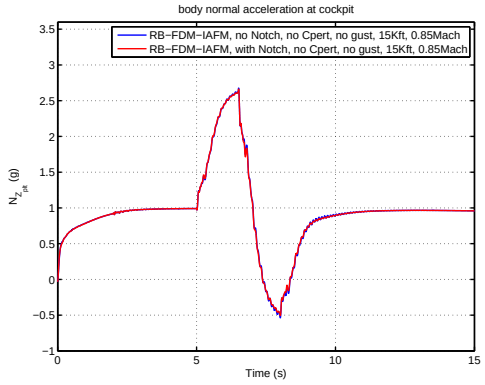

(a) Normal Accel. at Pilot Location, Nz_{Plt}.

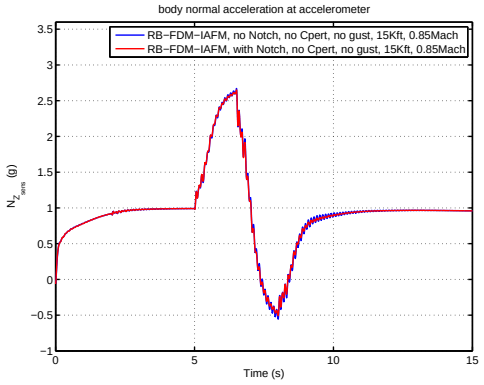

(b) Normal Accel. at Sensor Position, Nz_{SNS}.

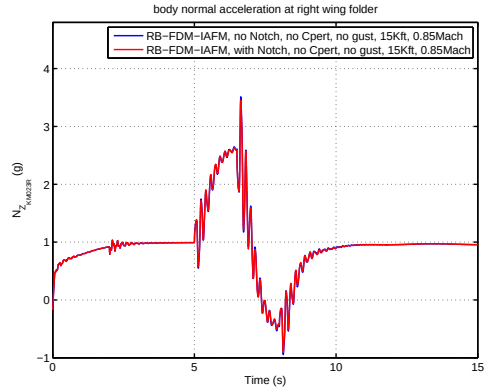

(c) Normal Accel. at Right Wing Folder Position, Nz_{km023R}.

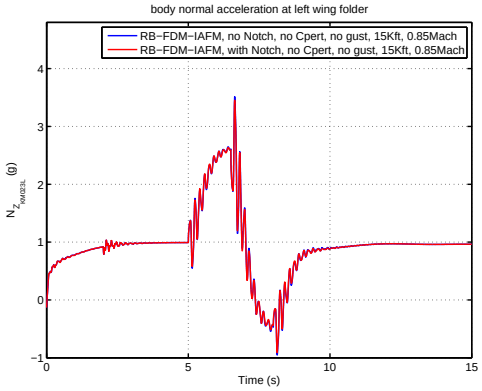

(d) Normal Accel. at Left Wing Folder Position, Nz_{km023L}.

Figure 6. Closed Loop Response of the Linear F/A-18 AAW Aeroelastic Model With/Without Notch Filters at M = 0.85, H = 15 Kft (Longitudinal Stick Command).

- The vibration responses induced by the 9.5 Hz aeroelastic mode are successfully suppressed with the use of the H_∞ feedback controller.
- The H_∞ feedback controller has little influence on the rigid dynamics response.
- The H_∞ feedback controller cannot reduce the vibration response of the normal acceleration at wing folder position, Nz_{km023R} and Nz_{km023L}.

Performance Validation of the H_∞ Controller at M = 0.95, H = 15 Kft

At flight simulation condition M = 0.90, H = 15 Kft, the simulation results with the feedback controller in the loop are plotted in Figures 15, 16, and 17. The simulation results obtained at M = 0.95, H = 15 Kft are similar as those at M = 0.85, H = 15 Kft and M = 0.90, H = 15 Kft.

Finally, a frequency domain comparison of aeroelastic/aeroservoelastic system with/without notch filter and with/without feedback controller in the loop is illustrated in Figure 18. Figure 18(a) shows bode plot of the aeroelastic/aeroservoelastic model from collective trailing edge flapron to the normal acceleration at Sensor Position, Nz_{sens} with and without notch filter, at M = 0.85. The aeroelastic/aeroservoelastic model is estimated using the system identification method. Figure 18(b) shows bode plot of the aeroelastic/aeroservoelastic model from collective trailing edge flapron to the normal acceleration at Sensor Position, Nz_{sens} with and without feedback controller, at M = 0.85. The similar comparisons are performed at other two flight conditions at M = 0.90 and M = 0.95. From these comparisons, it is observed that

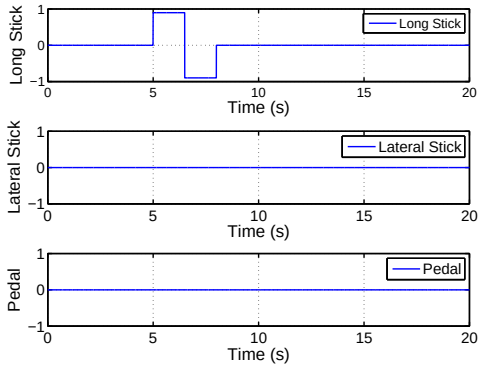

(a) Doublet Longitudinal Stick Command.

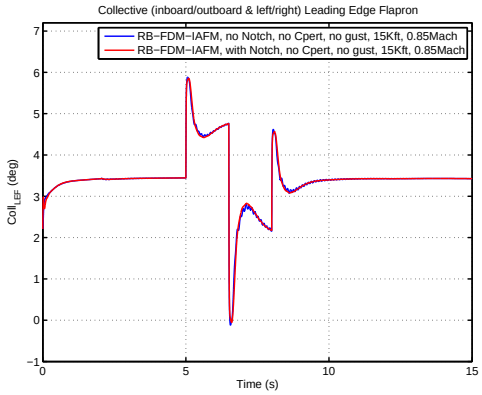

(b) Collective LEF, $Coll_{LEF}$.

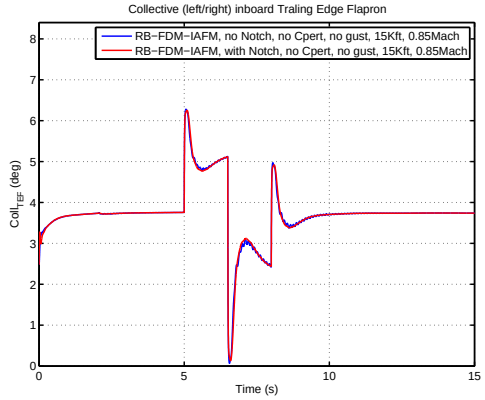

(c) Collective TEF, $Coll_{TEF}$.

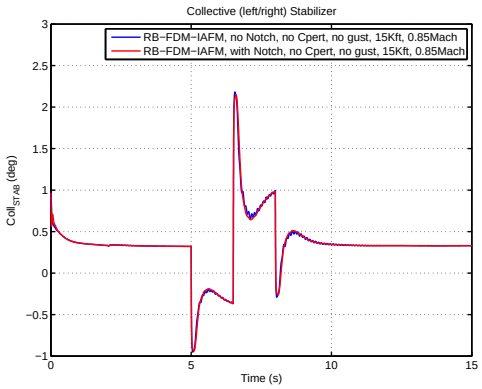

(d) Collective Stabilator, $Coll_{STAB}$.

Figure 7. Closed Loop Response of the Linear F/A-18 AAW Aeroelastic Model With/Without Notch Filter at M = 0.85, H = 15 Kft (Longitudinal Stick Command).

- If the frequency change of the elastic modes is small, the notch filter indeed helps to reduce the aeroelastic/aeroservoelastic mode interaction.
- It is feasible to apply the adaptive control algorithm for the suppression of the aeroelastic/seroservoelastic mode interaction instead of using notch filters.

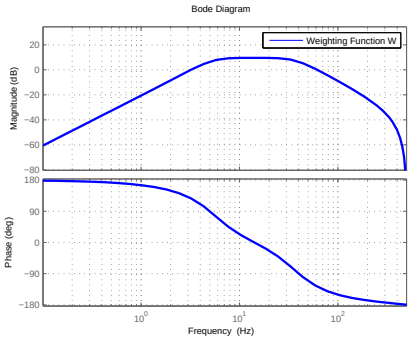

(a) Weighting Function W.

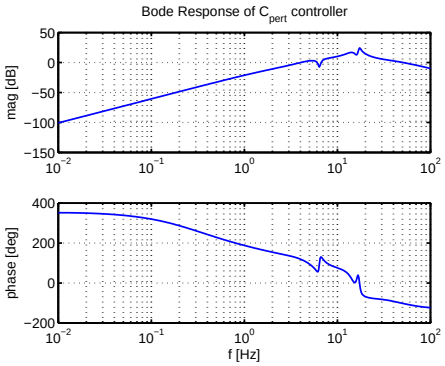

(b) Bode Plot of the Controller.

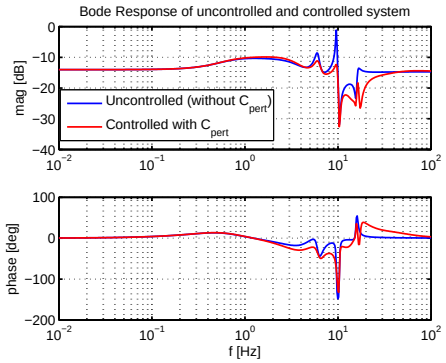

(c) Frequency Domain Comparison.

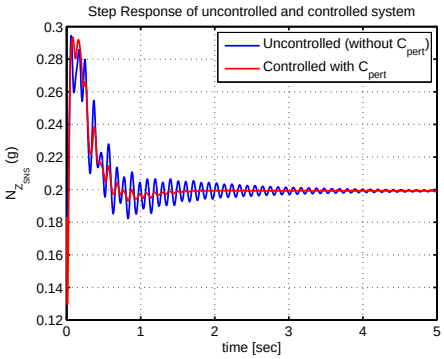

(d) Time Domain Comparison.

Figure 8. Results of the H_∞ Control Synthesis at M =0.85, H = 15 Kft (Using $Coll_{TEF}$ and Nz_{SNS} for Feedback Connection).

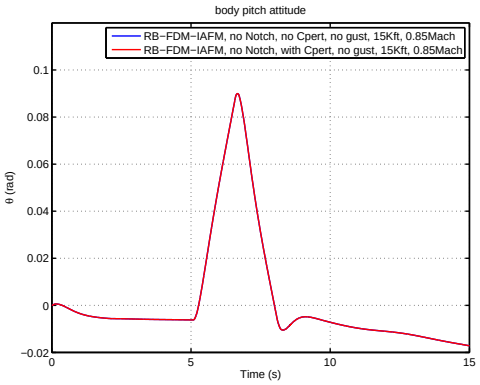

(a) Pitch Angle, $\theta(t)$.

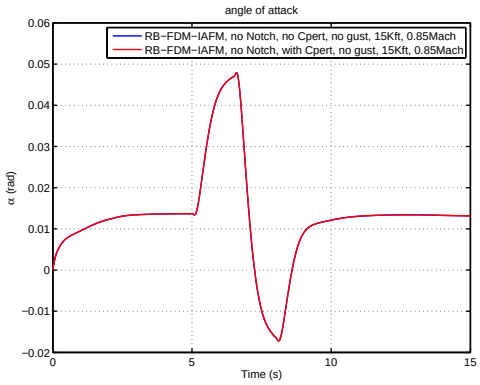

(b) Angle of Attach, $\alpha(t)$.

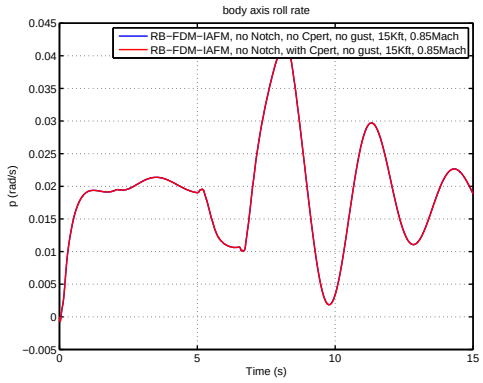

(c) Roll Rate, $p(t)$.

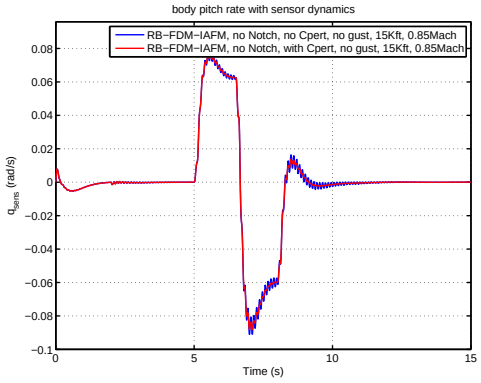

(d) Pitch Rate, $q(t)$.

Figure 9. Closed Loop Response of the Linear F/A-18 AAW Aeroelastic Model With/Without H_∞ Controller at M = 0.85, H = 15 Kft (Longitudinal Stick Command).

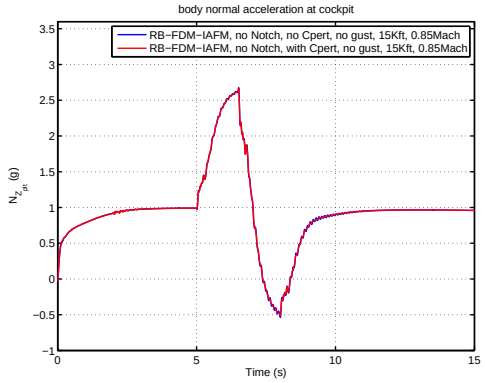

(a) Normal Accel. at Pilot Location, Nz_{Plt}.

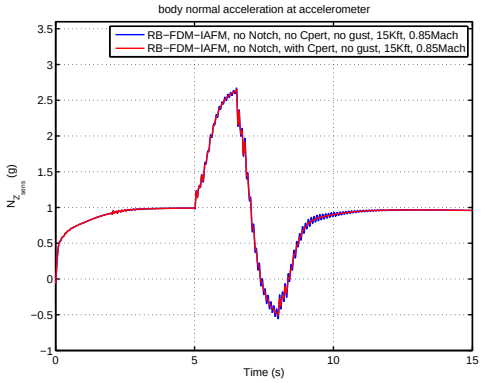

(b) Normal Accel. at Sensor Position, Nz_{SNS}.

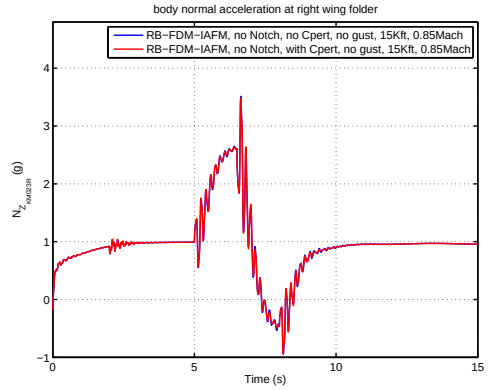

(c) Normal Accel. at Right Wing Folder Position, Nz_{km023R}.

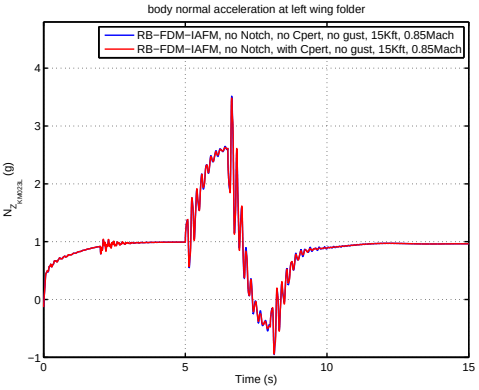

(d) Normal Accel. at Left Wing Folder Position, Nz_{km023L}.

Figure 10. Closed Loop Response of the Linear F/A-18 AAW Aeroelastic Model With/Without H_∞ Controller at M = 0.85, H = 15 Kft (Longitudinal Stick Command).

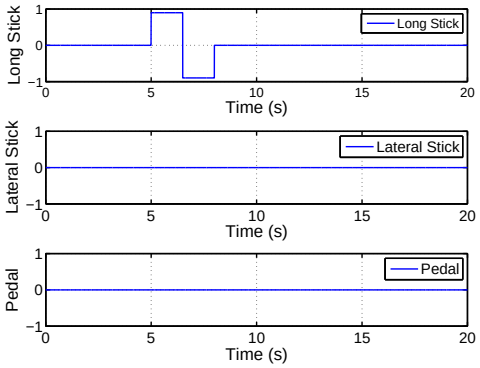

(a) Doublet Longitudinal Stick Command.

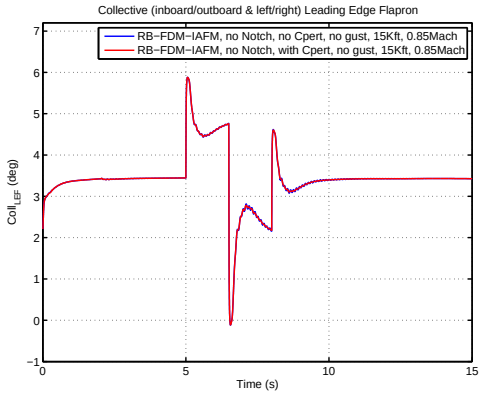

(b) Collective LEF, $Coll_{LEF}$.

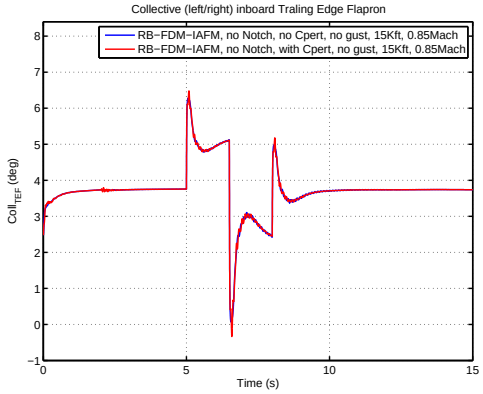

(c) Collective TEF, $Coll_{TEF}$.

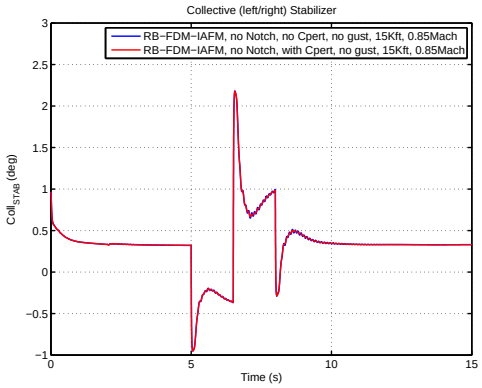

(d) Collective Stabilator, $Coll_{STAB}$.

Figure 11. Closed Loop Response of the Linear F/A-18 AAW Aeroelastic Model With/Without H_∞ Controller at M = 0.85, H = 15 Kft (Longitudinal Stick Command).

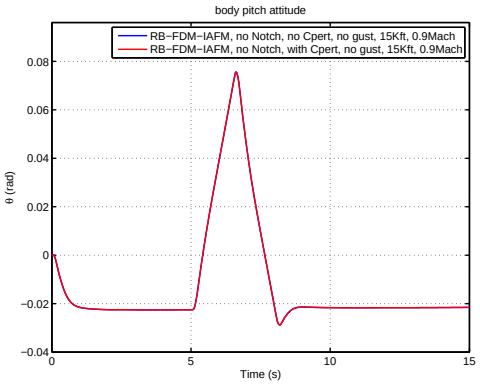

(a) Pitch Angle, $\theta(t)$.

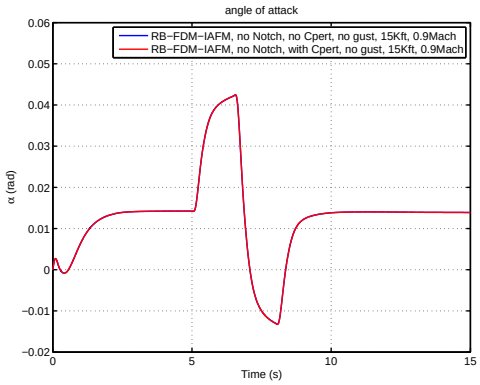

(b) Angle of Attach, $\alpha(t)$.

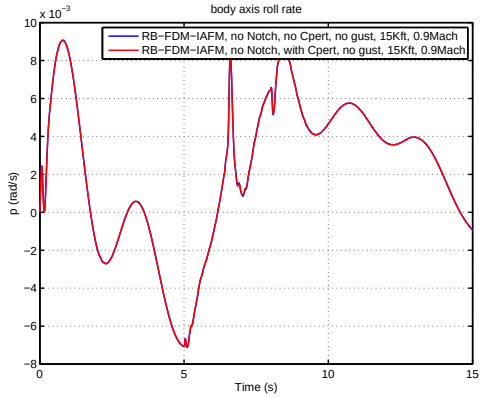

(c) Roll Rate, $p(t)$.

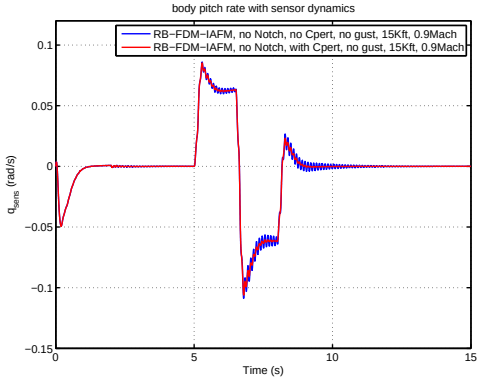

(d) Pitch Rate, $q(t)$.

Figure 12. Closed Loop Response of the Linear F/A-18 AAW Aeroelastic Model With/Without H_∞ Controller at M = 0.90, H = 15 Kft (Longitudinal Stick Command).

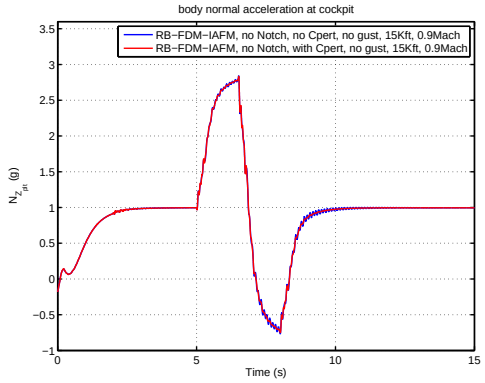

(a) Normal Accel. at Pilot Location, Nz_{Plt}.

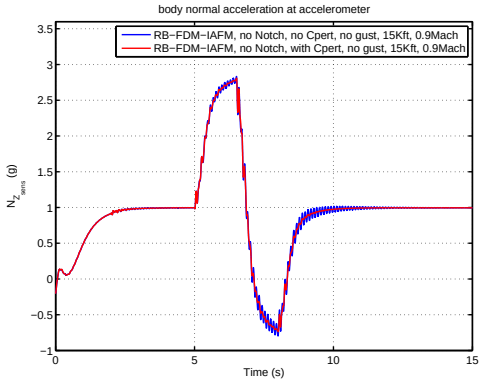

(b) Normal Accel. at Sensor Position, Nz_{SNS}.

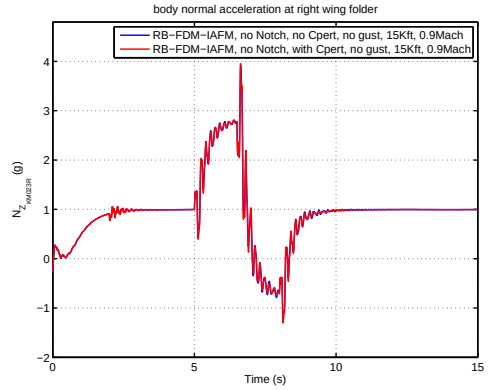

(c) Normal Accel. at Right Wing Folder Position, Nz_{km023R}.

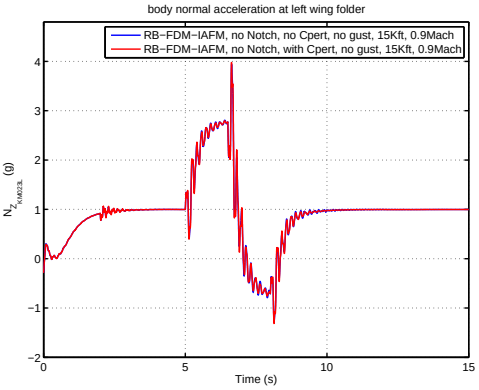

(d) Normal Accel. at Left Wing Folder Position, Nz_{km023L}.

Figure 13. Closed Loop Response of the Linear F/A-18 AAW Aeroelastic Model With/Without H_∞ Controller at M = 0.90, H = 15 Kft (Longitudinal Stick Command).

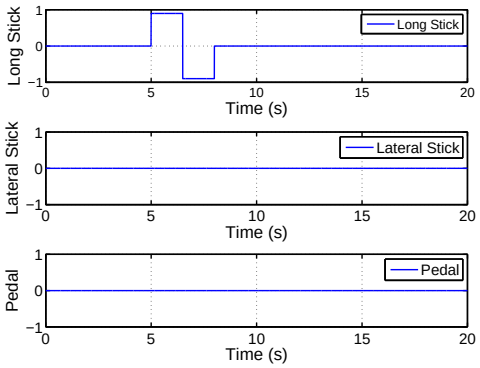

(a) Doublet Longitudinal Stick Command.

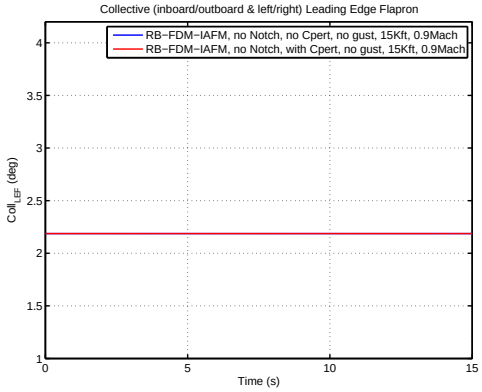

(b) Collective LEF, $Coll_{LEF}$.

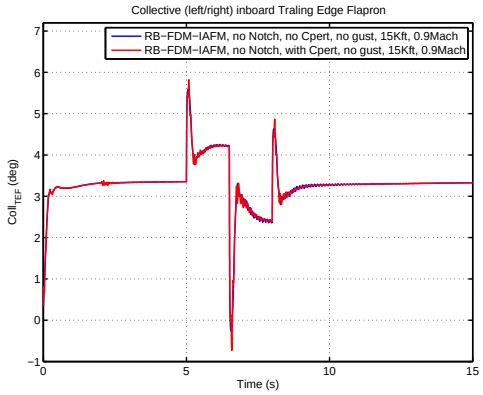

(c) Collective TEF, $Coll_{TEF}$.

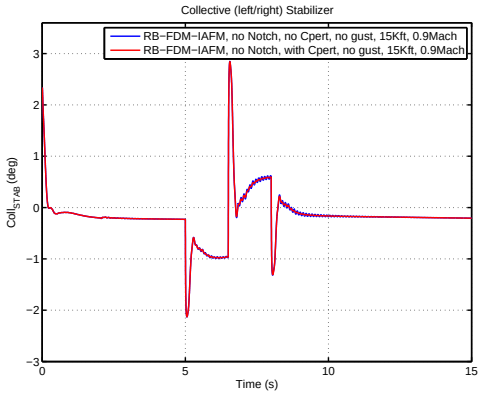

(d) Collective Stabilator, $Coll_{STAB}$.

Figure 14. Closed Loop Response of the Linear F/A-18 AAW Aeroelastic Model With/Without H_∞ Controller at M = 0.90, H = 15 Kft (Longitudinal Stick Command).

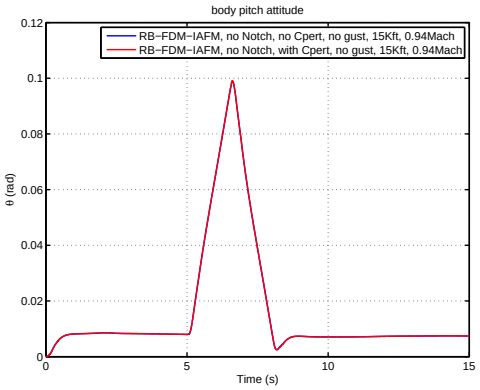

(a) Pitch Angle, $\theta(t)$.

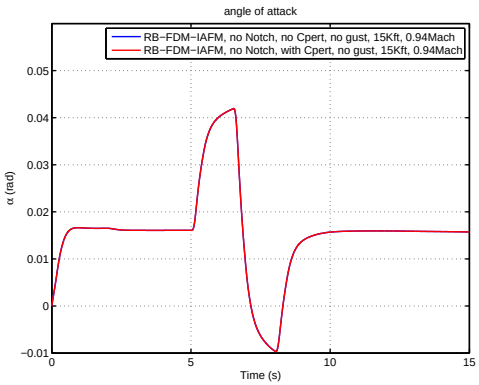

(b) Angle of Attach, $\alpha(t)$.

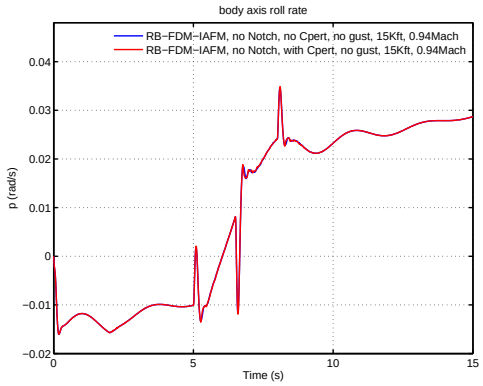

(c) Roll Rate, $p(t)$.

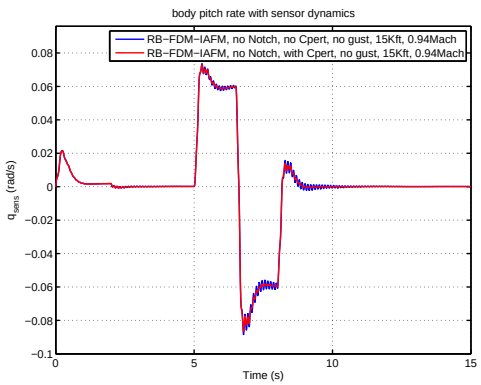

(d) Pitch Rate, $q(t)$.

Figure 15. Closed Loop Response of the Linear F/A-18 AAW Aeroelastic Model With/Without H_∞ Controller at M = 0.95, H = 15 Kft (Longitudinal Stick Command).

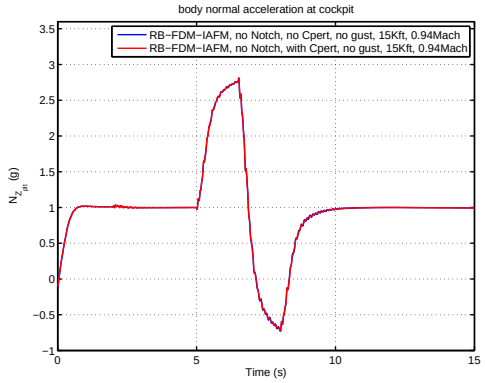

(a) Normal Accel. at Pilot Location, Nz_{Plt}.

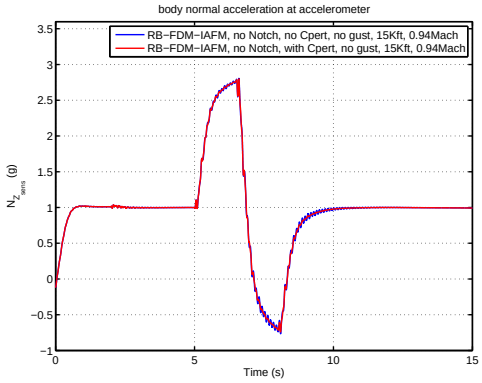

(b) Normal Accel. at Sensor Position, Nz_{SNS}.

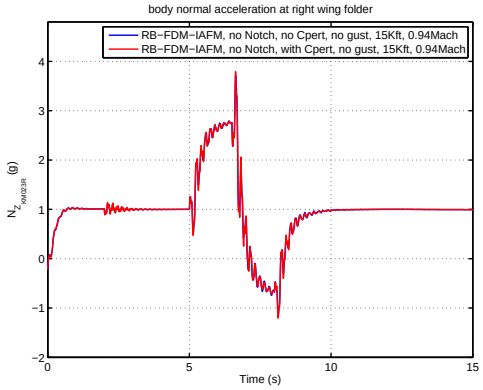

(c) Normal Accel. at Right Wing Folder Position, Nz_{km023R}.

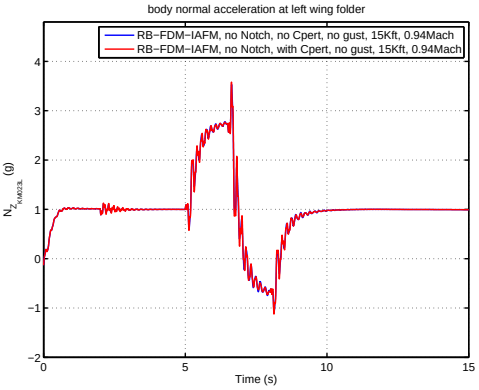

(d) Normal Accel. at Left Wing Folder Position, Nz_{km023L}.

Figure 16. Closed Loop Response of the Linear F/A-18 AAW Aeroelastic Model With/Without H_∞ Controller at M = 0.95, H = 15 Kft (Longitudinal Stick Command).

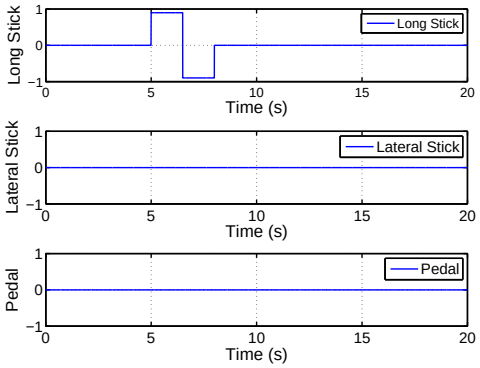

(a) Doublet Longitudinal Stick Command.

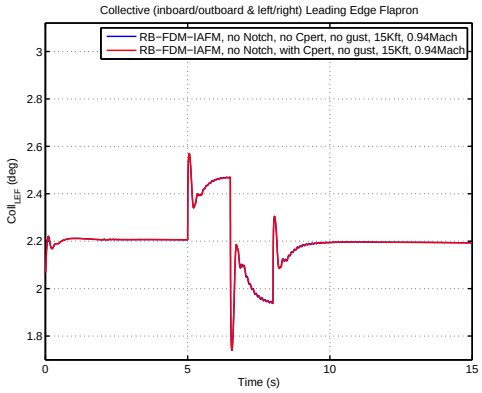

(b) Collective LEF, $Coll_{LEF}$.

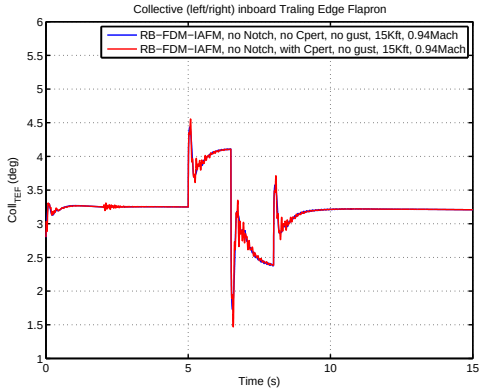

(c) Collective TEF, $Coll_{TEF}$.

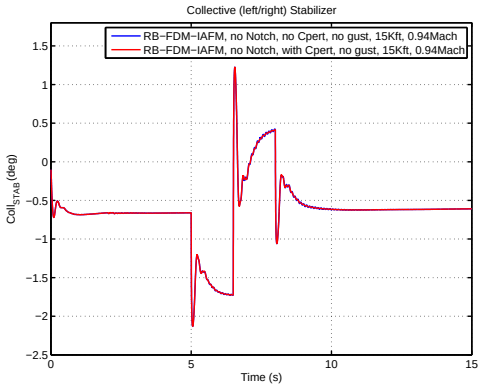

(d) Collective Stabilator, $Coll_{STAB}$.

Figure 17. Closed Loop Response of the Linear F/A-18 AAW Aeroelastic Model With/Without H_∞ Controller at M = 0.95, H = 15 Kft (Longitudinal Stick Command).

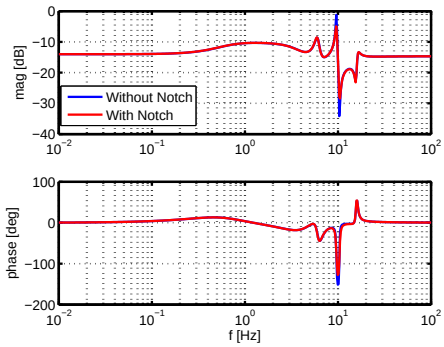

(a) Effect of Notch Filter at M = 0.85.

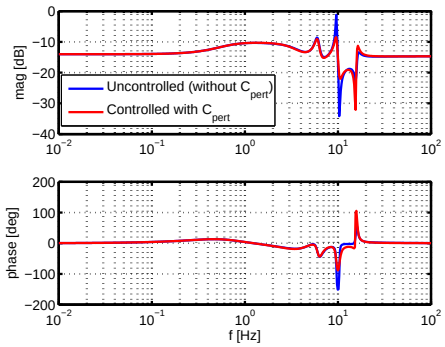

(b) Effect of Controller at M = 0.85.

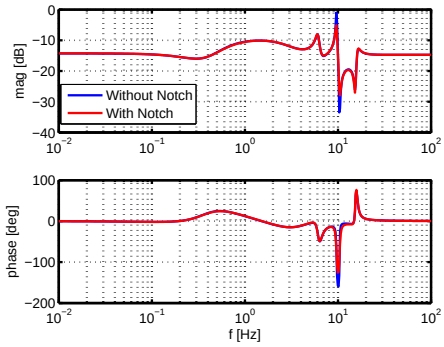

(c) Effect of Notch Filter at M = 0.90.

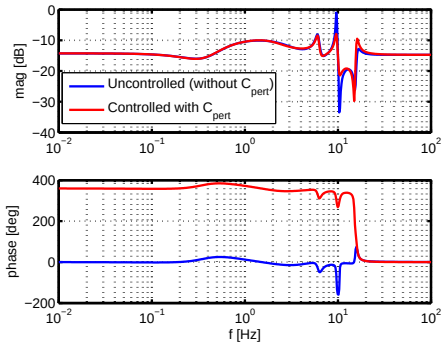

(d) Effect of Controller at M = 0.90.

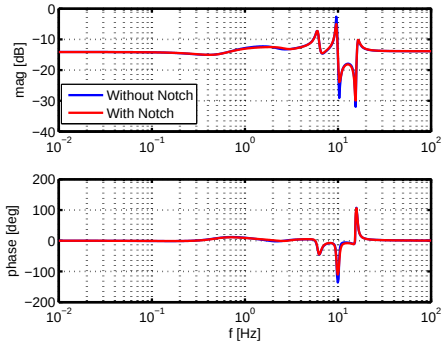

(e) Effect of Notch Filter at M = 0.95.

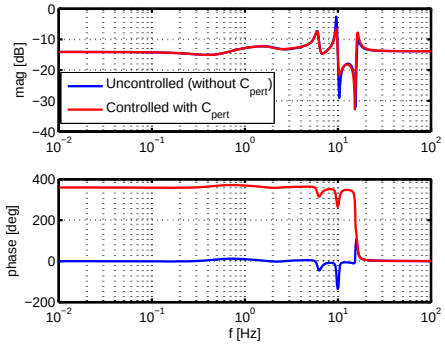

(f) Effect of Controller at M = 0.95.

Figure 18. Performance Comparison of the Notch Filter and Feedback Controller on Suppression of the Aeroelastic Modes Interaction.

V. Conclusions

In this paper, the possibility of applying an adaptive feedback control for the suppression of aircraft's structural vibration in the presence of any aeroelastic/aeroservoelastic interaction was investigated. In addition, the effectiveness of implementation of the notch filters in the flight control system for aeroelastic/aeroservoelastic vibration suppression was also studied. In the case that the change of the aircraft configuration is not significant, i.e., the frequencies of the flexible modes of the aircraft only have small changes, the non-adaptive notch filters shall work properly. On the other hand, with the proposed adaptive feedback control technology, the flexible dynamics can be consistently monitored and estimated via system identification algorithms, and its undesirable effects can be successfully minimized through a design of the robust feedback control law. Therefore, if the changes of the aircraft configuration are significant, the proposed adaptive feedback control outperforms the notch filters for the suppression of the aeroelastic/aeroservoelastic modes interaction.

Acknowledgments

Research is supported by NASA Dryden Flight Research Center under Small Business Innovation Research (SBIR) Phase II contract NNX09CB63C.

References

[1]Overschee, P. and de Moor, B., *Subspace Identifiction for Linear Systems:Theory-Implementation-Applications*, Kluwer Academic Publisher, Dordrecht, Belgium, 1996.

[2]de Callafon, R., Miller, D. N., Zeng, J., and Brenner, M. J., "Step Based Experiment Design and System Identification for Aeroelastic Dynamic Modeling," *AIAA Atmospheric Flight Mechanics Conference*, Chicago, IL, 2009, AIAA-2009-5707.

[3]Glover, K. and McFarlane, D., "Robust Stabilization of Normalized Coprime Factor Plant Descriptions with H_∞–Bounded Uncertainty," *IEEE Trans. on Automatic Control, AC–34*, 1989, pp. 821–830.